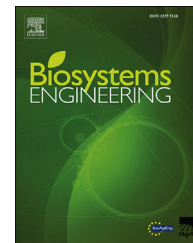




ELSEVIER

Available online at www.sciencedirect.com

ScienceDirect

journal homepage: www.elsevier.com/locate/issn/15375110

Research Paper

A CFD study on improving air flow uniformity in indoor plant factory system



Ying Zhang, Murat Kacira*, Lingling An

Department of Agricultural and Biosystems Engineering, The University of Arizona, Tucson, AZ, USA

ARTICLE INFO

Article history:

Received 23 January 2016

Received in revised form

17 April 2016

Accepted 22 April 2016

Published online 12 May 2016

Keywords:

Boundary layer

CFD

Lettuce

Plant factory

Tipburn

Uniformity

Indoor plant factories are one of the alternative ways to meet the demands of food production for the increased urban dwellers. It enables growers to grow food crops consistently and locally with high quality. In an indoor plant factory, a forced convection based ventilation and circulation system is used to control the growing environment and maintain climate uniformity. Lettuce is a common leafy crop grown in indoor plant factories and an improper design could cause the tip burn of lettuces which usually occurs at inner and newly developing leaves with low transpiration rate due to the existence of a stagnant boundary layer under high transpiration demand. A three-dimensional computational fluid dynamics (CFD) model was developed and validated through simulating the growing environment in a single shelf production system. An improved air circulation system was designed and proposed to help providing a dynamic and uniform boundary layer which could help preventing tip burn occurrences in lettuce production. A perforated air tube with three rows of air jets was designed to provide vertical air flow down to the crop canopy surface. Four cases with the perforated air tubes were compared with a control treatment. The results indicated that the case with two perforated air tubes was able to provide an average air velocity of 0.42 m s^{-1} with a coefficient of variation of 44%, which was recommended as the optimal design of air circulation system among four cases in this study.

Published by Elsevier Ltd on behalf of IAGrE.

1. Introduction

Population expansion, climate change, and limited natural resources all require the development of innovative agricultural technologies to meet the rising global demand for food and agricultural sustainability. Controlled environment agriculture (CEA) combines various agricultural technologies and enables growers to control environmental variables to optimise crop growing systems, crop yield and quality, as well

resource use efficiency (Jones, 2005). As a new form of CEA, an indoor plant factory is typically placed in a multi-story building or a warehouse around an urban area. It enables growers to grow crop consistently year around and locally with high food quality (Kozai, 2013; Kozai, Chun, & Ohyama, 2004).

In indoor plant factories, ventilation systems play an important role to replace air in the controlled environment food production systems to provide favourable growing

* Corresponding author.

E-mail address: mkacira@email.arizona.edu (M. Kacira).<http://dx.doi.org/10.1016/j.biosystemseng.2016.04.012>

1537-5110/Published by Elsevier Ltd on behalf of IAGrE.

Nomenclature

ρ	fluid density (kg m^{-3})
t	time (s)
x	Cartesian coordinates (m)
i	Cartesian coordinates index
u	Velocity component (m s^{-1})
j	Cartesian coordinates index
δ	Kronecker delta
μ	dynamic viscosity ($\text{kg m}^{-1} \text{s}^{-1}$)
g	acceleration due to gravity (m s^{-2})
C_a	specific heat capacity ($\text{W kg}^{-1} \text{K}^{-1}$)
T	temperature (K)
S_T	thermal sink or source (W m^{-3})
E	heat load (W)
h	convection heat transfer coefficient ($\text{W m}^{-2} \text{K}^{-1}$)
T_s	surface temperature (K)
T_∞	fluid temperature (K)
q''_{cond}	conductive heat transfer rate (W m^{-2})
k	thermal conductivity coefficient ($\text{W m}^{-1} \text{K}^{-1}$)
q''_{rad}	radiant heat flux (W m^{-2})
ε	Emissivity
σ	Stefan–Boltzmann constant ($\text{W m}^{-2} \text{K}^{-4}$)
q	volumetric heat generation (W m^{-3})
q''_{conv}	convective heat flux (W m^{-2})
V_{hs}	heat source volume (m^3)
u_{out}	outlet air velocity (m s^{-1})
Q	outlet flow rate ($\text{m}^3 \text{s}^{-1}$)
A_{out}	outlet opening area (m^2)
K_s	roughness height (m)
C_s	roughness constant
h_c	height of the crop (m)

environment and desirable air movement. The importance of airflow control for promoting the photosynthesis and transpiration of plants has been demonstrated by previous research (Kitaya, Tsuruyama, Shibuya, Yoshida, & Kiyota, 2003; Korthals, Knight, Christianson, & Spomer, 1994; Shibuya & Kozai, 1998). Compared to the maturity of ventilation technologies for greenhouses, few studies have been conducted to study ventilation, climate and air flow uniformity characteristics in an indoor plant factory and the design guidelines are still lacking. The improper design of air conditioning and air distribution systems in an indoor plant factory can cause non-uniform environmental condition and airflow patterns, leading to non-uniform crop growth, uneven quality and crop disorders.

Tip burn in lettuce crop is a calcium deficiency induced disorder and it is characterized by browning margins in lettuces (Aloni, Pashkar, & Libel, 1986; Shear, 1975). It usually occurs at inner and newly developing leaves with low transpiration rate due to the existence of a stagnant boundary layer under high transpiration demand conditions (Barta & Tibbitts, 1991; Clarkson, 1984). In order to prevent or reduce lettuce tip burn, one of the methods is to increase air supply to the leaf surfaces of lettuce. The principle is to enhance the

transpiration rate of lettuce by accelerating air movement at leaf surface to decrease the boundary layer resistance both at leaf or at crop canopy scale (Downs & Krizek, 1997; Fitter & Hay, 1981; Yabuki, 1990). Kitaya (2005) reported the effect of air velocity (horizontal direction) less than 1.3 m s^{-1} on the net photosynthetic rate and transpiration rate on a seedlings canopy and single leaves of cucumber. For the cucumber seedlings canopy, the net photosynthetic rate and transpiration rate increased respectively by 1.2 and 2.8 times when the air velocity was increased from 0.02 to 1.3 m s^{-1} . For the single leaves of cucumber, the net photosynthetic rate and transpiration rate increased respectively by 1.7 and 2.1 times when the air velocity was increased from 0.005 to 0.8 m s^{-1} . The results showed that enhancing the wind velocity has a positive effect on photosynthesis and transpiration. The promotions of the net photosynthetic rate and transpiration rate by enhancing air velocity (horizontal direction) around crops for other crops were also reported, such as a dwarf–rice plant canopy with air current speed increased from 0.01 to 0.8 m s^{-1} (Kitaya, Tsuruyama, Kawai, Shibuya, & Kiyota, 2000) and sweet potato leaves with air current speed increased from 0.01 to 1 m s^{-1} (Kitaya et al., 2003). The effects of providing horizontal airflow to lettuce for preventing tipburn in an indoor plant factory were studied (Lee et al., 2013). Although a stable horizontal airflow of 0.28 m s^{-1} significantly reduced the incidence of tip burn of lettuce, tip burn was still detected in the inner leaves near harvest at the centre of the cultivation bed, where there was high light intensity and less air flow due to the enclosure effect of outer leaves (Chang & Miller, 2004). Compared to horizontal airflow, vertical airflow is more effective for suppressing the occurrence of tip burn by blowing airflow into the lower and inner part of leaves (Goto & Takakura, 1992; Shibata, Iwao, & Takano, 1995). Vertical downwards air currents with airspeeds higher than 0.3 m s^{-1} around plants were suggested for promoting the photosynthetic and transpiration rates of plants in plant culture systems (Kitaya et al., 2000).

Interactions of environmental variables in a multi-layer indoor plant factory system are complex involving a number of physical and chemical properties of overall system and various system configurations that are challenging to model numerically, time consuming and cost prohibitive. Computational fluid dynamics (CFD) has been shown to be an effective tool in simulating physical complex phenomena with reasonable accuracy and analysing environmental uniformity in controlled environments. The CFD technology has been shown to be an effective and mature tool to be used in controlled environment agriculture for analysing aerodynamics, and climate and complex fluid phenomena (Baeza et al., 2009; Bournet, Ould Khaoua, & Boulard, 2007; Fatnassi, Poncet, Bazzano, Brun, & Bertin, 2015; Fidaros, Baxevanou, Bartzanas, & Kittas, 2010; Lee & Short, 2000; Majdoubi, Boulard, Fatnassi, & Bouirden, 2009; Tamimi, Kacira, Choi, & An, 2013). Therefore, it was decided to investigate if CFD could be an effective engineering tool to evaluate and enhance system designs for improved air conditioning and microclimate uniformity within multi-tier crop growing systems.

The objectives of this study contain 1) to develop a validated three dimensional CFD model to simulate growing environment in a single shelf production system, and 2) to

design and propose an improved air circulation system that can provide a desired average uniform airspeed of $0.3\text{--}1\text{ m s}^{-1}$ at the crop canopy surface level to help preventing lettuce tip burn in the production shelf system.

2. Materials and methods

2.1. Experimental setup for model validation

In this study, numerical simulations have been conducted to verify the capability of CFD to predict air velocity and temperature distribution in a single shelf of a multi-tier food production system equipped with a forced ventilation system and with fluorescent lamps (energy source). The experiment for model validation study was performed on a single shelf of a small multi-tier vertical food production system prototype as a test-bed with dimensions of 0.46 m (Width) \times 0.86 m (Length) \times 0.33 m (Height). Two fluorescent lamps (901621-T5, 24 W, Spectralux, Sunlight Supply Inc., Vancouver, WA, USA) were installed in an aluminium housing with a reflector at the centre area close to the ceiling of the shelf. Four exhaust fans (Ari flow: $0.013\text{ m}^3\text{ s}^{-1}$, AD0812LB-A70GL, ADDA, Mouser Electronics, Mansfield, TX, USA) were placed evenly (with the distance between the centres of two neighbouring fans set at 0.21 m) on the back side wall. One air inlet ($0.14\text{ m W} \times 0.33\text{ m H}$) on front side wall was created as a pressure-inlet. Two hot-wire anemometers (FMA-905-V-R, Range: $0\text{--}25\text{ m s}^{-1}$, Accuracy: $\pm 1.5\%$ of full scale at room temperature, OMEGA Engineering, Stamford, CA, USA) were used to measure average horizontal air speed at five different coordinates with different heights and distances to the exhaust fans (Fig. 1). Fine thermocouples (T-type) were used to

measure the average surface temperature on the lamp surface (3 points) and on the reflector (1 point) and the air temperature (the point close to the exhaust fans) (Fig. 1). Two capacitance sensors (HMP60, Measurement range: $-40\text{ }^\circ\text{C}$ to $+60\text{ }^\circ\text{C}$, Accuracy: $\pm 0.6\text{ }^\circ\text{C}$, Vaisala, Woburn, MA, USA) were used to measure air temperature and relative humidity (Measurement range: $0\text{--}100\%$ non-condensing, Accuracy at $0\text{ }^\circ\text{C}$ to $+40\text{ }^\circ\text{C}$: $\pm 3\%$ RH ($0\text{--}90\%$ Relative Humidity)) at two points (Fig. 1). All sensors were connected to a data logger (CR 1000, Campbell Scientific, Logan, UT, USA). Surface temperature data were recorded every second for 5 min, air temperature/relative humidity data were recorded every second for 15 min, as with the airspeed. For each measurement, the data were averaged and were used for comparisons between measured and CFD simulated data.

2.2. CFD model

A commercial CFD software (FLUENT, Ver. 16.1, ANSYS Inc., Canonsburg, PA) was used for simulations. The fluid flow in the problem domain was assumed to be a steady-state, incompressible, and three dimensional turbulent flow. The numerical calculation of airflow can be considered as mathematical formulations of the conservation laws of fluid mechanics. By applying the mass, momentum, and energy conservation, the fundamental governing equations of fluid dynamics; the mass (1), momentum (Navier–Stokes) (2), and energy (3) equation can be written as follows (Norton & Sun, 2006):

$$\frac{\partial \rho}{\partial t} + \frac{\partial}{\partial x_i} (\rho u_i) = 0 \quad (1)$$

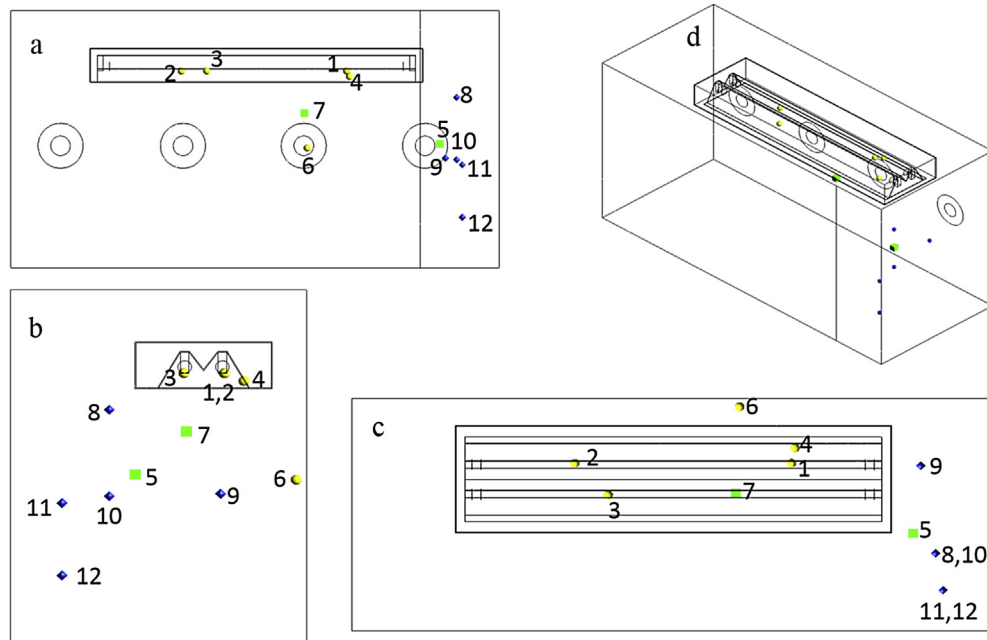


Fig. 1 – Sensor locations for measurements a) Front view b) Side view c) Top view d) 3D view of the prototype production shelf. ● = hot wire anemometer (air velocity), ◆ = fine thermocouple (lamp surface temperature), ■ = capacitance sensor (air temperature and RH).

$$\frac{\partial}{\partial t}(\rho u_i) + \frac{\partial}{\partial x_j}(\rho u_i u_j) = \frac{\partial}{\partial x_i} \left[-\rho \delta_{ij} + \mu \left(\frac{\partial u_i}{\partial x_j} + \frac{\partial u_j}{\partial x_i} \right) \right] + \rho g_i \quad (2)$$

$$\frac{\partial}{\partial t}(\rho C_a T) + \frac{\partial}{\partial x_j}(\rho u_j C_a T) - \frac{\partial}{\partial x_j} \left(\lambda \frac{\partial T}{\partial x_j} \right) = S_T \quad (3)$$

The two-equation k-epsilon model was employed to compute the contributions of turbulence to the mean flow by solving two additional governing equations for turbulent kinetic energy (κ) and turbulent dissipation (ϵ). It is one of the most common two equation models for specifying a turbulent flow (Jiru & Bitsuamlak, 2010). This model has been widely used in agricultural engineering (Bustamante et al., 2013) as well as in describing the turbulent nature of fluid flow in greenhouse models (Bourmet et al., 2007; Kacira, Sase, & Okushima, 2004; Kim et al., 2008; Mistriotis, Bot, Picuno, & Scarascia-Mugnozza, 1997; Rohdin & Moshfegh, 2007; Tamimi et al., 2013). In this study, the realizable k-epsilon model was used to compute the turbulent effect of air flow. This turbulence model has shown substantial improvements over the standard k-epsilon model where the flow features include strong streamline curvature, vortices, and rotation (Posner, Buchanan, & Dunn-Rankin, 2003; Shih, Liou, Shabbir, Yang, & Zhu, 1994) and has shown to be more accurate for predicting the spreading rate of both planar and round jets (Fluent User's Guide, 2012), which is the case in the current study with the jets created by the perforated air tube design. It is also likely to provide superior performance for flows involving rotation, boundary layers under strong adverse pressure gradients, separation, and recirculation (Shih et al., 1994). The realizable k-epsilon model has been successfully used to simulate indoor wall-bounded air flows for ventilation system design in a mushroom house (Han et al., 2009) and airflow pattern in a plant factory (Lim & Kim, 2014).

3. Numerical simulation: model validation

3.1. Numerical model and boundary conditions

A three-dimensional computational model was created based on the measured dimensions of a single prototype production shelf. There are three heat transfer mechanisms for the T5 fluorescent lamps in the model: convection, conduction, and radiation. The energy use efficiencies of lamps vary between different models and manufacturers (Thimijan & Heins, 1983). Thimijan and Heins (1983) reported that for a 46 W of cool-white fluorescent lamp, 22 W of energy was lost by heat and 14 W of energy was emitted as thermal radiation. Thus, 78% of total energy was converted into heat and about 50% of total energy was lost through conduction and convection. Similarly, Gilani, Montazeri, and Blocken (2013) defined light bulbs as energy source with 50% of total power used for heat generation. In the boundary conditions, the heat loss due to convection was set at lamp surfaces. The heat loss due to infrared radiation and conduction from the lamps was assigned to the top wall of the shelf and the wall of the canopy surface. The heat source with 50% of total power lost by volumetric convection from T5 fluorescent lamp surface was

defined as the energy term with a constant heat generation of 114,833 W m⁻³ according to Eq. (4) (Gilani et al., 2013):

$$q = \frac{E}{V_{hs}} \quad (4)$$

where q is the volumetric heat generation (W m⁻³), E is the heat load (W), and V_{hs} is the heat source volume (m³).

Table 1 summarises the boundary conditions and the numerical parameters used for three-dimensional CFD simulation. The operating air temperature for the simulations was set to 297 K which was the air temperature in the room where the experiments were conducted. The thermal properties of glass for the fluorescent lamp and aluminium for the lamp housing, the reflector and the shelf were defined and assigned to the walls according to the material properties (Table 2). The walls were assumed to be smooth. Since the air temperature difference in the shelf is small, the Boussinesq approximation for airflow was used in order to achieve a faster convergence (Lau & Liu, 2003). This approximation assumes that the air density is constant and it considers the influence of buoyancy on air movements in the momentum equation. The air velocity as boundary condition at the exhaust fan was set to 3.1 m s⁻¹, based on the volumetric flow rate of the fan, and it was calculated as:

$$u_{out} = \frac{Q}{A_{out}} \quad (5)$$

where u_{out} is the air velocity (m s⁻¹) at the exhaust fan boundary, Q is the outlet volumetric flow rate (m³ s⁻¹), and A_{out} is the outlet opening area (m²).

The computational grid had 593,511 cells with three-dimensional elements of combined tetrahedron, pyramid, and hexahedron meshing. A finer mesh was imposed near the fluorescent lamps and exhaust fans, where the thermal and pressure gradients were steeper. Furthermore, mesh quality was confirmed by evaluating the skewness (0.3 ± 0.1), aspect ratio (1.9 ± 0.5), and orthogonal quality (0.8 ± 0.1) to improve accuracy and stability of numerical computations.

3.2. Solver settings

In this study, the SIMPLE algorithm was used for pressure-velocity coupling (Patankar, 1980). For spatial discretisation, least square cell based scheme was employed for gradient term. The standard scheme was applied for the pressure term. First order discretisation schemes were used for momentum, energy and viscous terms of the governing equations for a better convergence of calculations (Mirade & Daudin, 2006). The convergence criterion was set to 10⁻⁶ on energy term and 10⁻³ on all other terms to evaluate if the solution is converged or not.

4. Numerical simulation: design of air circulation system for a single cultivation shelf

4.1. Geometry of the computational model

The computational model for an air circulation system design with dimensions 1.52 m (W) × 1.52 m (L) × 0.3 m (H) was

Table 1 – Boundary conditions summary for CFD simulations for model validation.

Fluid: Air ^a		
Operating air temperature in the production domain: 297 K		
Gravitational acceleration: 9.81 m s ⁻²		
Energy source (T5 fluorescent lamps): 114,833 W m ⁻³		
Models	Property	
Energy model	Activated	
Viscous model	Realizable k-epsilon model with standard wall functions and full buoyancy effect	
Parameter	Boundary conditions	Property
Exhaust fans	Velocity-inlet	3.1 m s ⁻¹
Inlet-vent	Pressure-inlet	Gauge pressure: 0 Pa
Lamp-wall	Wall	Thermal property of glass ^b
Lamp housing, reflector, shelf walls	Wall	Thermal property of aluminium

^a From Doxon (2007).

^b From Brunberg and Aspelin (2011).

Table 2 – Thermal properties of matter used in the CFD model.

Thermal property	Air	Glass	Plastic	Leaf	Aluminium
Density (kg m ⁻³)	1.225	2500	1430	1078	2719
Specific heat (J kg ⁻¹ K ⁻¹)	1005	830	1150	3100	871
Thermal conductivity (W m ⁻¹ K ⁻¹)	2.53 × 10 ⁻³	1.3	0.52	0.55	202.4
Dynamic viscosity (kg m ⁻¹ s ⁻¹)	1.783 × 10 ⁻⁵				
Thermal expansion coefficient (K ⁻¹)	3.43 × 10 ⁻³				

created based on the size of a representative single shelf from a commercial scale indoor plant factory with the width of 1.52 m and a height of 0.3 m from the top wall to the lettuce canopy surface. Because the replicated phenomenon for fluid flow along the shelf was expected in this study, the model was assumed to be a slice of the shelf with the length of 1.52 m. Two side walls of the shelf were defined as symmetry walls in the simulations. In order to achieve a desired photosynthetic photon flux density of 230 $\mu\text{mol m}^{-2} \text{s}^{-1}$ at the bottom wall of the geometry (assumed to be crop canopy surface level), eight T8 fluorescent lamps (T8, 32W, Photon flux: 48 $\mu\text{mol s}^{-1}$, Philips) for a production area of 1.74 m² were added and evenly distributed in the model with the distance of 0.15 m between the centreline of two neighbouring lamps.

In order to enhance air movement and to help preventing tip burn symptoms of lettuces in an indoor plant factory, inserting relevant parallel lines on the existing lighting systems close to the top wall to provide a vertical air flow to crop canopy surface was recommended as one of the methods of installing an air flow apparatus (Lee et al., 2013). A polyethylene perforated air tube was designed as part of the air circulation system to provide vertical air flow to lettuce canopy surface in this study. The target air current speed at the canopy surface was set between 0.3 m s⁻¹ (Kitaya et al., 2000) and 1 m s⁻¹ (Wells & Amos, 1994).

The perforated polyethylene air tube had a diameter of 0.05 m with a length of 1.52 m based on the layout and size of the shelf. Instead of placing an air tube between each two lamps, a perforated air tube with three rows of jets was designed for a wider airflow coverage at the canopy surface. Although the aperture ratio, defined as the total hole area to the tube cross-sectional area, less than 1.5 is suggested to

have a uniform air jet along perforated air tube (Wells & Amos, 1994), the small diameter of air tube restricts the application of this principle with. A smaller aperture ratio for a fixed diameter of a perforated tube means that a decreased hole size or decreased number of holes with increased distance between two holes has to be applied for having a smaller total hole area. This can also cause a non-uniform air flow distribution at the target surface due to possible stagnant air zones between two holes where air jets from the tube cannot reach. Therefore, the design of the perforated air tube was adjusted by changing aperture ratio and maintaining the space between two holes to be no less than 1.5 times of the maximum hole diameter, so that this would also help preventing a weakened air tube (Wells & Amos, 1994). A final design of the perforated air tube with the aperture ratio of 1.9 is shown in Fig. 2. The perforations were extended with the length of 0.017 m in order to correct the air jets angles so that they were almost perpendicular to the floor. The air tube had seventeen sets of evenly spaced perforations numbered from one to seventeen (one being the closest to the inlet). Each of these sets was 0.076 m from the next and consisted of three holes which were placed at 30° from each other. The sets from one to eleven had hole diameter of 0.01 m and the diameter for the remaining sets of holes was 0.009 m. The distance from the first hole to the tube head and the last hole to the end of the tube was 0.05 m.

Five cases were studied and compared in this study (Fig. 3): Case 0 – control treatment (no air supply, flow is driven by natural convection); Case 1 – one air tube; Case 2 – two air tubes with same air flow direction (distance between two pipes: 0.59 m); Case 3 – two air tubes with reversed airflow direction (distance between two pipes: 0.59 m), and Case 4 –

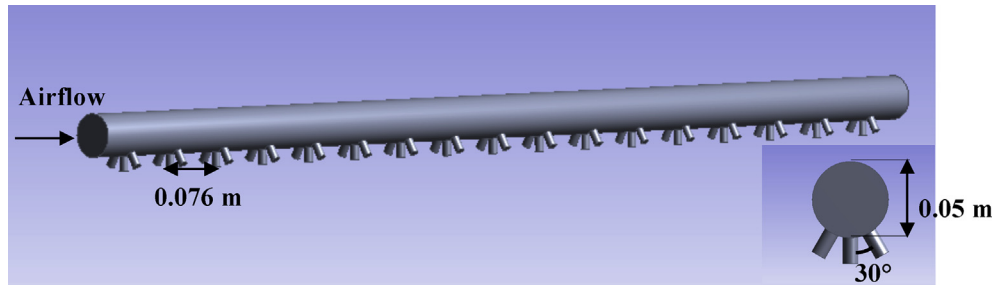


Fig. 2 – Proposed overhead perforated air tube design.

four air tubes with same air flow direction. The same methods were used to generate the computational mesh for each case.

4.2. Numerical model and boundary conditions

The computational grids for each case had around 3.5 million of cells with three-dimensional elements of combined tetrahedron, pyramid, and hexahedron meshing. Finer meshes were imposed near the fluorescent lamps and perforated air tubes, where the thermal or pressure gradients were steeper. Table 3 shows the boundary conditions and the numerical parameters used for three-dimensional CFD simulation. It was assumed that the initial operating air temperature in the production domain was 297 K in an indoor plant factory. The temperature of cool air injected into the air tubes was set to 288 K. The gravitational effect was included and the Boussinesq approximation for airflow was applied. The energy source from T8 fluorescent lamps was calculated according to Eq. (4) with the assumption that 50% of the total power input was lost as convective heat from the lamp surfaces (Gilani et al., 2013; Thimijan & Heins, 1983). The other 50% was assigned to the wall surfaces at the shelf. It was assumed that the wall surface temperature had the same temperature as the initial temperature of surrounding air, which was 294 K. The thermal properties of glass, aluminium, and a polyethylene air tube were assigned to the walls according to the material properties (Table 2). The top wall of the shelf was assumed to be smooth. The roughness effects for turbulent flow were assigned with roughness height (K_s) and a roughness constant (C_s) for the wall representing the lettuce canopy surface at the bottom of the problem domain. The roughness constant $C_s = 0.5$ represents a uniform roughness at the wall surface. The roughness height (m) for lettuce was calculated according to Eq. (6) (Alves, Perrier, & Pereira, 1998):

$$K_s = 0.126h_c \quad (6)$$

where h_c is the height of crop canopy (m) and the value $h_c = 0.15$ was used.

Combinations of hexahedron and tetrahedron mesh were used in the simulations. Finer meshes were imposed near the fluorescent lamps and perforated air tubes. Furthermore, for all cases mesh quality was confirmed by evaluating the skewness, aspect ratio, and orthogonal quality to improve accuracy and stability of numerical computations. The values of mesh quality for skewness, aspect ratio, and orthogonal quality were 0.2 ± 0.1 , 1.9 ± 0.5 , and 0.9 ± 0.1 , respectively.

4.3. Solver settings

The SIMPLE algorithm was used for pressure–velocity coupling (Patankar, 1980). For spatial discretization, a least square cell based scheme was employed for gradient term. Second order discretisation schemes were used for pressure, momentum and energy term for more accurate results compared to first order discretization schemes. First order upwind discretisation schemes were used for viscous terms of the governing equations for a better convergence of calculations because of the problem of transient characteristics of the airflow. The convergence criterion was 10^{-6} on the energy, momentum, and continuity term and 10^{-3} on the viscous term (Mondaca & Choi, 2014) to monitor the residuals and to confirm whether a solution is converged or not.

5. Results and discussions

5.1. Numerical simulation: model validation

The simulated air temperature, surface temperature and air velocity at twelve points were compared to those corresponding points from the experimental measurements in the single shelf interior domain. Model prediction accuracy was evaluated by comparing the percentage errors for each individual points between the measured and simulated data (Table 4). The results indicated that the prediction accuracy of 3D CFD model for air temperature and air velocities were with the average percentage errors of 8.9% and 7.5%, respectively, when compared to measured values. Airflow patterns within the system were also traced using a smoke generator (Smoke pencil, Chimney Balloon, Mauldin, Hampshire, UK) and the air flow was recorded using a digital camera. Similar air flow patterns were observed between the flow patterns generated by the smog generator and those obtained from the CFD simulation (data not shown).

5.2. Numerical simulation: design of air circulation system

5.2.1. Combining data for average velocity

The air flow uniformity at the lettuce canopy surface was evaluated with the coefficient of variation (CV). The CV is defined as the ratio of the standard deviation to the mean. The CV indicates the extent of variability in relation to the mean of the population. Therefore, a low value indicates a lower

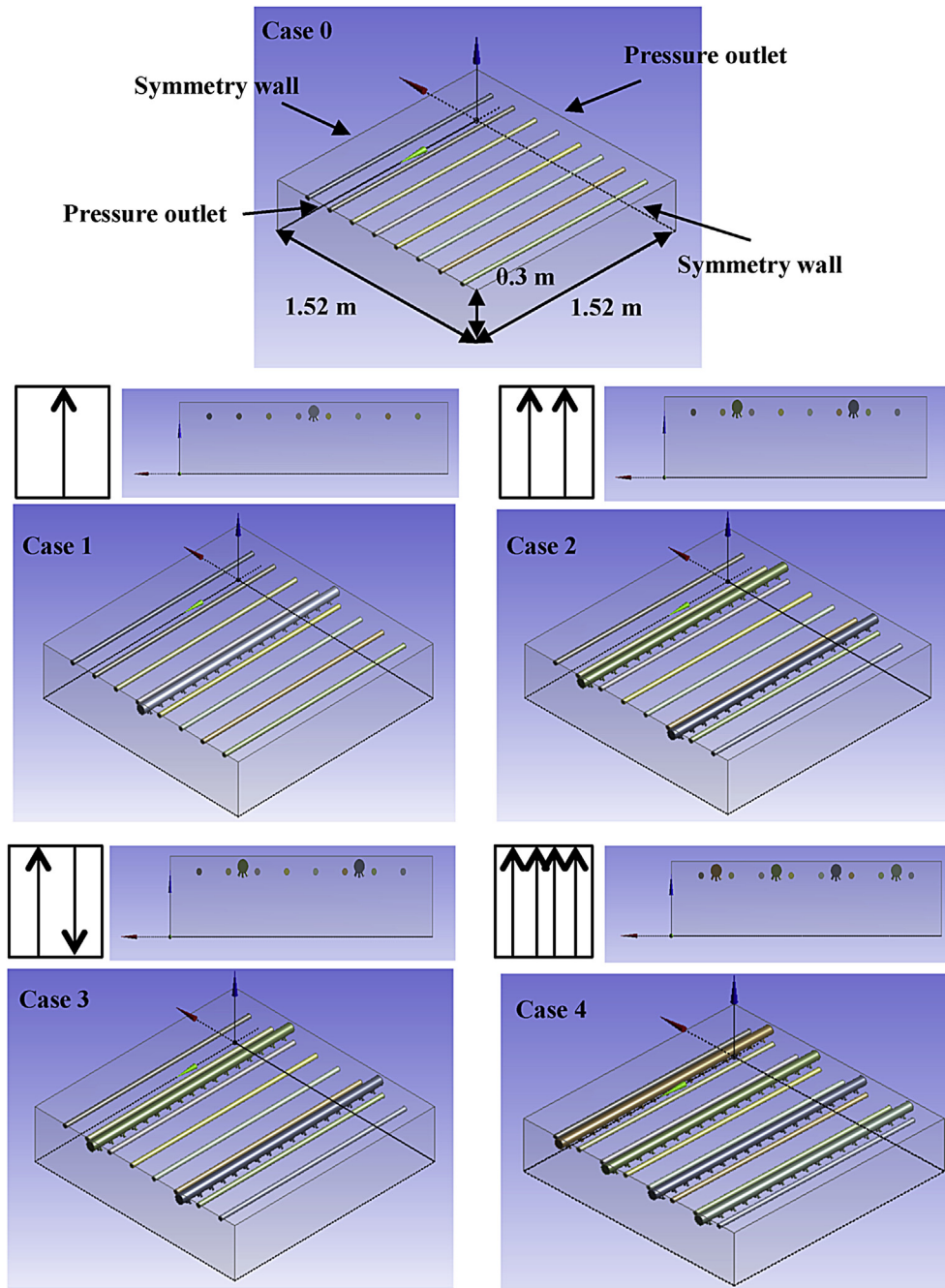


Fig. 3 – Cases with 3D computational model for air circulation system design: a) Case 0 with only natural convection no air tube, b) Case 1 with only single perforated air tube, c) Case 2 with two perforated air tube with the same direction for air flow, d) Case 3 with two perforated air tube with the flow in opposite direction, e) Case 4 with four perforated air tubes with the same flow direction.

variability in the data set. The air velocity at canopy surface lower than 0.3 m s^{-1} or higher than 1 m s^{-1} should be avoided in the shelf for lettuce crop in a multi-tier production system. Therefore, this criterion was used to assess the goodness of the designs by evaluating the percentages of cells in total at canopy surface with air velocities falling into this range. Thus, the average air velocities at the crop canopy surface plane in the simulation domain were calculated using 20,000 cells located at crop canopy surface in each case. The values of the

maximum air velocity, the minimum air velocity, the average air velocity, the percentage of cells with air velocity lower than 0.3 m s^{-1} , the percentage of cells with air velocity between 0.3 and 1 m s^{-1} , the percentage of cells with air velocity higher than 1 m s^{-1} , and the coefficient of variation for four cases with perforated air tubes are present in the [Table 5](#).

Although the smaller size of air jet outlet at the closed end of the air tube improved the general airflow uniformity along the perforated air tube, a slight difference in air velocity closed

Table 3 – Boundary conditions summary for CFD simulation for air circulation system design cases.

Fluid: Air ^a		
Operating air temperature in the production domain: 297 K		
Gravitational acceleration: 9.81 m s ⁻²		
Energy source (T8 fluorescent lamps): 25,912 W m ⁻³		
Models	Property	
Energy model	Activated	
Viscous model	Realizable k-epsilon model with standard wall functions and full buoyancy effect	
Parameter	Boundary conditions	Property
Air-tube inlet	Velocity-inlet	8 m s ⁻¹
Shelf-two-side-wall-1	Pressure-outlet	Gauge pressure: 0 Pa
Shelf-two-side-wall-2	Symmetry	Default
Lamp-wall	Wall	Thermal property of glass ^b
Air-tube-wall	Wall	Thermal property of plastic ^b
Shelf-top-wall	Wall	Thermal property of aluminium
Shelf-bottom-wall	Wall	roughness height: 0.019 m, roughness constant: 0.5

^a From Doxon (2007).

^b From Brunberg and Aspelin (2011).

Table 4 – Summary of simulated and measured data for model validation.

Point #	Measured lamp surface temperature (°C)	Simulated lamp surface temperature (°C)	Percentage error (%)
1	35.7 ± 0.3	37.0	3.6
2	52.9 ± 2.2	60.5	14.4
3	48.8 ± 2.2	56.9	16.6
4	27.3 ± 1.9	25.0	8.4
	Measured Air Temperature (°C)	Simulated Air Temperature (°C)	Percentage Error (%)
5	26.1 ± 0.6	24.1	7.7
6	25.8 ± 0.5	23.9	7.4
7	25.0 ± 0.3	24.0	4.0
	Measured Air velocity (m s ⁻¹)	Simulated Air velocity (m s ⁻¹)	Percentage Error (%)
8	0.78 ± 0.08	0.73	6.4
9	0.78 ± 0.09	0.70	10.3
10	0.49 ± 0.17	0.55	12.2
11	0.81 ± 0.06	0.78	3.7
12	0.81 ± 0.09	0.77	4.9

to the two ends of the air tube was still observed due to the nonlinearly increased static pressure along the air tube (Fig. 4). Therefore, the results showed that the design of the perforated air tube has effect on the air flow distribution at crop canopy surface. The air velocity contour diagrams at crop canopy surface were generated for each case (Fig. 5).

Without supplying any air into the shelf with flow mainly under natural convection (Case 0), the air velocities at crop canopy surface were stagnant and close to zero. A small air

circulation and slightly higher air velocities compared to the centre of the shelf (still close to zero air velocities) were observed towards the edges of the production shelf. This slow airflow and circulation is mainly induced by air temperature difference and air density gradient caused by the heat generated from the fluorescent lamps. In Case 1 with one air tube, the highest air velocity was observed at the centre of the shelf. With the three rows of air jets, at crop canopy surface, 68% of the cells can achieve the air velocity higher than 0.3 m s⁻¹. The average air velocity at crop canopy surface was 0.41 ± 0.21 m s⁻¹ and the coefficient of variation was 51%. The stagnant areas with air velocity lower than 0.1 m s⁻¹ were observed along the margins of the shelf, as well as the stagnant zone at the inter-jet spacing.

Case 2 and Case 3 were designed to improve the air velocity at the stagnant areas in Case 1. A compensation effect using the reversed direction of air tubes in Case 3 was expected to improve the air flow uniformity at the lettuce canopy surface. With the increased volumetric flow rate, a higher momentum exchange between air jets and quiescent fluid helped to decrease the stagnant areas and have a more uniform air flow distribution. From the results, a smaller stagnant area and a more uniform airflow distribution were observed with two air tubes in Case 2 and Case 3 with coefficients of variation of 44% and 46%, respectively. Based on the values analysed from 20,000 cell points on the crop canopy surface, the percentage of cells with air velocity lower than 0.3 m s⁻¹ was decreased from 32% to 26% in Case 2 and 28% in Case 3. The percentage of cells with air velocity higher than 1 m s⁻¹ was increased up to 10%. In general, the average air velocity in Case 2 and Case 3 was 0.42 ± 0.19 m s⁻¹. The percentages of cells with air velocity between 0.3 and 1 m s⁻¹ were 64% and 66%, respectively. Due

Table 5 – Summary of air velocity at crop canopy surface for each case in the design of air circulation system.

	MAX (m s ⁻¹)	MIN (m s ⁻¹)	AVG (m s ⁻¹)	PCT (<0.3 m s ⁻¹)	PCT (0.3–1 m s ⁻¹)	PCT (>1 m s ⁻¹)	CV
Case 1	1.02	0.01	0.41	32%	67%	<1%	51%
Case 2	1.27	0.02	0.42	26%	64%	10%	44%
Case 3	1.15	0.03	0.42	28%	66%	6%	46%
Case 4	0.73	0.02	0.28	59%	41%	0%	45%

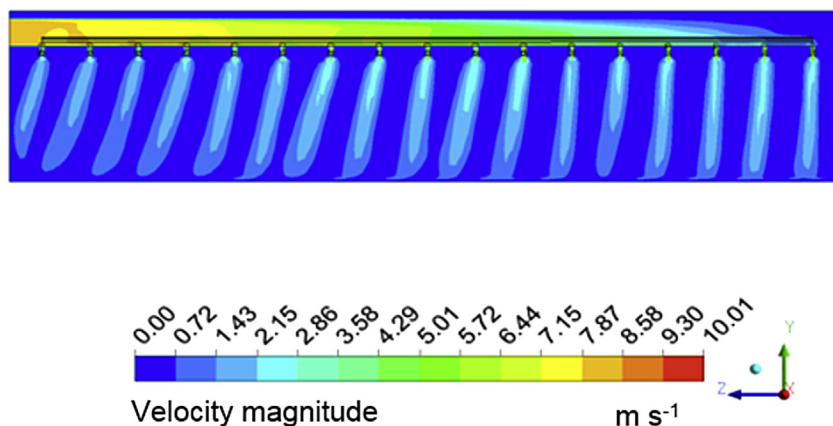


Fig. 4 – Air jets distribution and pattern along the perforated air tube.

to the non-normality of the data, a non-parametric method, the Wilcoxon signed rank test, was used for testing whether samples from Case 2 and Case 3 originate from the same distribution. The results showed that there is no difference (p -value = 0.72) between Case 2 and Case 3 in terms of air velocity at significant level of $\alpha = 0.05$. The slightly higher coefficient of variation in Case 3 showed that the reversed direction of air flow in air tubes cannot help to improve the overall air flow uniformity at the canopy surface.

With four perforated air tubes as in Case 4, the smaller distance between two air tubes restricted the development of air jets and caused a more turbulent air flow at canopy surface. The smallest average air velocity (0.28 m s^{-1}) and maximum air velocity (0.73 m s^{-1}) at canopy surface were generated compared to other cases. With the decreased average air velocity, more than half of the cells (59%) had the air velocity lower than the target lower limit air velocity of 0.3 m s^{-1} . For air flow uniformity, Case 4 had no significant improvement compared to Case 2 and Case 3 with the coefficient of variation of 45%.

5.2.2. Air jets interaction

Figure 6 showed the cross sectional air velocity contour diagrams at central plate crossing the fluorescent lamps, where two side ends were defined as symmetry walls. For Case 0, a stagnant air with nearly constant air velocity close to zero was observed in the production shelf. For the four cases with perforated air tubes, the range of air velocity was defined as $0\text{--}1.3 \text{ m s}^{-1}$ to visualize the air velocity distribution at canopy boundary layer. The multi-jet configurations were affected by two types of interactions: the jet-to-jet interaction between adjacent jets prior to the air jets onto the canopy surface and the interaction between the air jets and the flow formed by the spent air of the neighbouring jets (Weigand & Spring, 2009). The latter dominated the air flow distribution in the air circulation system. For instance, the stagnant zones in the four cases were mainly caused by the jet-to-jet interference, which occurred between the adjacent rows of air jet at one air tube and between two air tubes. When two developed air jets conflicted with each other, with the obstacle of the canopy surface, the airflow moved upward and formed a circulating air flow pattern and zone between two perforated tube

sections. The stagnant zones between each pair of rows of air jet were observed at merged points.

6. Conclusions

A 3D CFD model was developed to simulate growing environment in a single shelf production system and to design and propose an improved air circulation system that provide a desired average air current speed at the crop canopy surface level as an alternative approach to help preventing lettuce tip burn and contribute to achieving a more uniform air current speeds at the canopy. A perforated air tube installed between supplemental lighting fixtures in the production shelf was designed and proposed to enhance vertical air flow to crop canopy surface. The designs of air circulation system with perforated air tubes were able to improve the air movement at crop canopy surface compared to the control treatment with only natural convection driven air flow. The three rows of air jets on the perforated air tube helped to expand the coverage of air flow at crop canopy surface from one single tube. The design as described in Case 2, applying two perforated air tubes in the shelf, is recommended based on the system evaluated in the current study, because it resulted in smaller stagnant zones on the crop canopy surface and achieved more uniform air flow distribution, with the CV of 44% in Case 2 and 46% in Case 3 compared to 51% in Case 1. From the economics point of view with materials, installation and energy demand, the design in Case 2 would be a better design option. In addition, the reversed direction of air tubes in Case 3 did not improve the airflow uniformity. Although Case 4 had the similar air flow uniformity at the canopy surface, the average air velocities were much lower than 0.3 m s^{-1} . With two air tubes, the average velocity of 0.42 m s^{-1} can be achieved at the crop canopy surface. Compared to an air circulation system with horizontal fans, the multi-jet perforated air tube can help to overcome the enclosure effect of outer leaves and push air down to the crop canopy surface, especially at the centre of the cultivation bed. Based on the overall comparison, the two air tube design as described in Case 2 is recommended for the shelf system evaluated in this study. Since the air flow pattern and air velocities created on the crop canopy surface depend

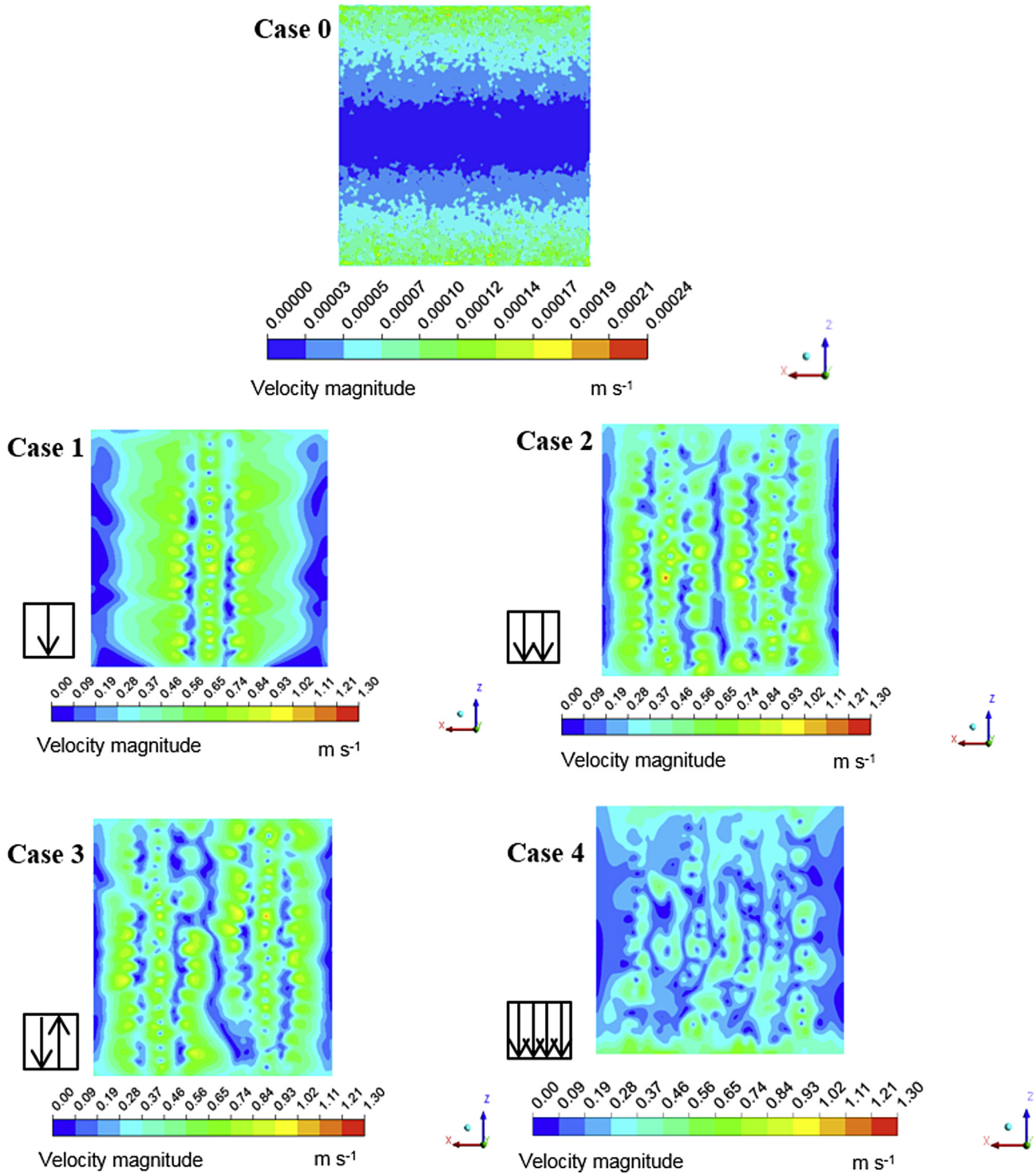


Fig. 5 – Air velocity contour diagrams at crop canopy surface.

on the air jet angle, total number of holes, and position of air jets further combination and detailed analysis is also recommended to refine the conceptual design proposed in this study.

This study illustrated the ability of CFD as an engineering design tool to predict airflow in a ventilated indoor environment and demonstrated the concept of using perforated air tube for the design of the air circulation system in an indoor

plant factory. Further research is necessary to improve the design of the perforated air tubes for potential use in multi-tier crop production systems. Alternative designs can integrate combinations of vertical, diagonal, and horizontal airflow combinations to improve air flow patterns and uniformity and to achieve desired air velocities. Instead of using a perforated air tube design, the ceiling of the production shelf can be designed in a way to provide vertical air flows on the

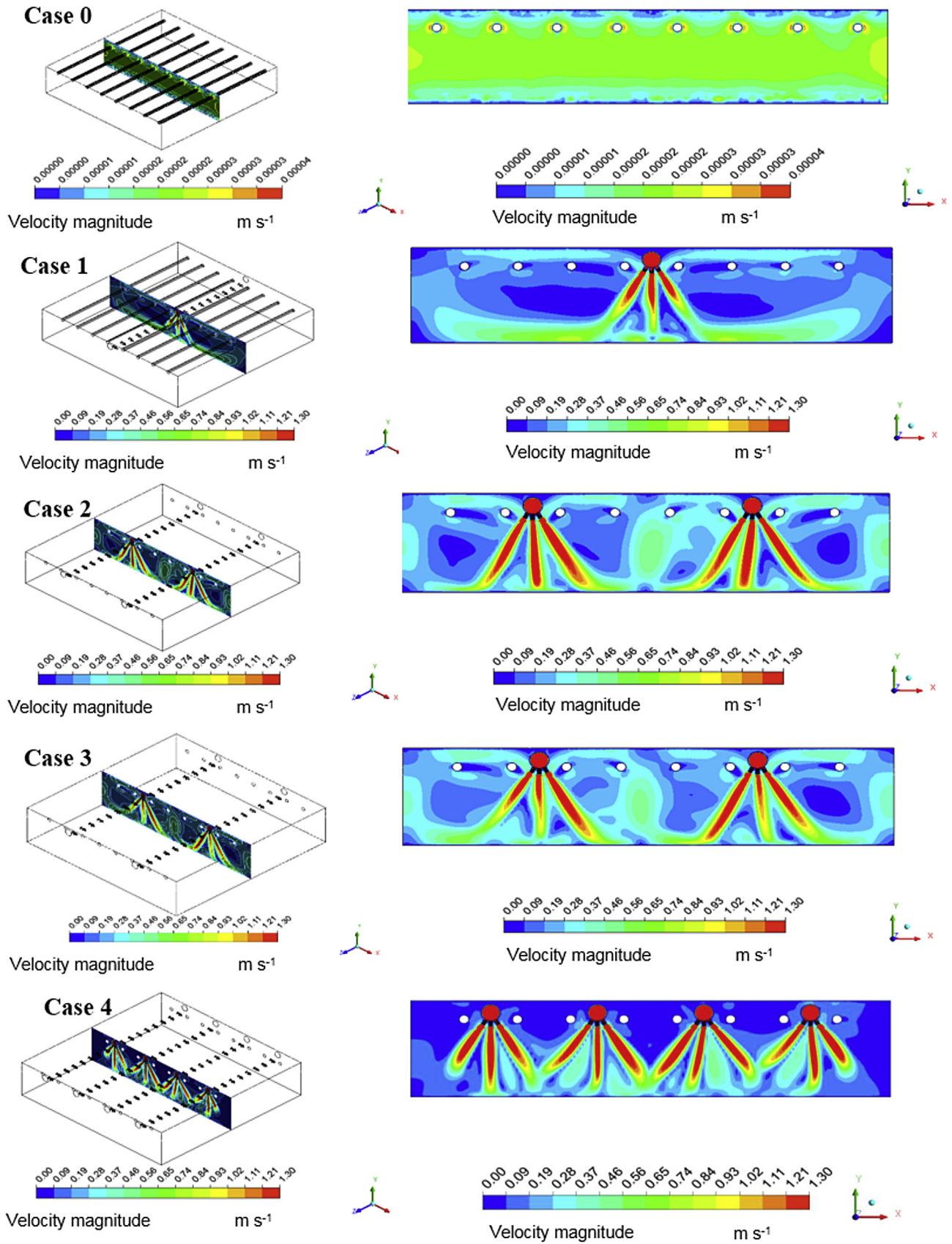


Fig. 6 – Air velocity contour diagrams at central plate in the production shelf.

crop canopy. A more comprehensive study including sub-models can be conducted, such as: (1) a porous media model to simulate the ways that a crop canopy will affect airflow, (2) a radiation model to incorporate the effect of sole-source lighting systems heat and light input into the production system and on the crop canopy, and (3) an evapotranspiration model to include latent and sensible heat exchanges between crop canopy and the surrounding air, and (4) discrete phase model to account for CO₂ distribution. Such a comprehensive model can help to study key design features and variables in further detail and to recommend design optimisation leading to improved resource use efficiency in indoor plant factory based multi-tier food production systems. Our research is ongoing to develop such complex and integrated CFD models to study environments and various air conditioning and distribution system design concepts for potential use in indoor plant production systems.

REFERENCES

- Aloni, B., Pashkar, T., & Libel, R. (1986). The possible involvement of gibberellins and calcium in tipburn of Chinese cabbage: study of intact plants and detached leaves. *Journal of Plant Growth Regulation*, 4(1), 3–11.
- Alves, I., Perrier, A., & Pereira, L. S. (1998). Aerodynamic and surface resistance of complete cover crops: how good is the “big leaf”? *Journal of American Society of Agricultural Engineers*, 41(2), 345–351.
- Baeza, E. J., Pérez-Parra, J. J., Montero, J. I., Bailey, B. J., López, J. C., & Cázqueza, J. C. (2009). Analysis of the role of sidewall vents on buoyancy-driven natural ventilation in parallel-type greenhouses with and without insect screens using computational fluid dynamics. *Biosystems Engineering*, 104(1), 86–96. <http://www.sciencedirect.com/science/journal/15375110/104/1>.
- Barta, D. J., & Tibbitts, T. W. (1991). Calcium localization in lettuce leaves with and without tipburn: comparison of controlled-environment and field-grown plants. *Journal of the American Society for Horticultural Science*, 116, 870–875.
- Bournet, P. E., Ould Khaoua, S. A., & Boulard, T. (2007). Numerical prediction of the effect of vent arrangements on the ventilation and energy transfer in multi-span glasshouse using a bi-band radiation model. *Biosystems Engineering*, 98, 224–234.
- Brunberg, J., & Aspelin, M. (2011). *CFD modelling of headlamp condensation*. Sweden: Department of Applied Mechanics, Chalmers University of Technology.
- Bustamante, E., García-Diego, F.-J., Calvet, S., Estellés, F., Beltrán, P., Hospitaler, A., et al. (2013). Exploring ventilation efficiency in poultry buildings: the validation of computational fluid dynamics (CFD) in a cross-mechanically ventilated broiler farm. *Energies*, 6, 2605–2623.
- Chang, Y. C., & Miller, W. B. (2004). The relationship between leaf enclosure, transpiration, and upper leaf necrosis on Lilium ‘Star Gazer’. *Journal of the American Society for Horticultural Science*, 129, 128–133.
- Clarkson, D. T. (1984). Calcium transport between tissues and its distribution in the plant. *Plant Cell & Environment*, 7, 449–456.
- Downs, R. J., & Krizek, D. T. (1997). Air movement. In R. W. Langhans, & T. W. Tibbitts (Eds.), *Plant growth chamber handbook* (pp. 87–104). No. 340, Iowa Agr. & Home Econ. Expt. Sta. Spec. Rpt. No. 99, Ames, IA: North Central Regional Res. Publ.
- Doxon, J. C. (2007). *The shock absorber handbook* (2nd ed., p. 375). Hoboken, NJ: John Wiley & Sons, Ltd.
- Fatnassi, H., Poncet, J., Bazzano, M. M., Brun, R., & Bertin, N. (2015). A numerical simulation of the photovoltaic greenhouse microclimate. *Solar Energy*, 120, 575–584.
- Fidaros, D. K., Baxevanou, C. A., Bartzanas, T., & Kittas, C. (2010). Numerical simulation of thermal behavior of a ventilated arc greenhouse during a solar day. *Renewable Energy*, 35, 1380–1386.
- Fitter, A. H., & Hay, R. K. M. (1981). *Environmental physiology of plants* (3rd ed.). San Diego, CA: Academic Press, A Division of Harcourt Inc.
- Fluent User's Guide. (2012). Version 13.1. Canonsburg, PA: ANSYS, Inc.
- Gilani, S., Montazeri, H., & Blocken, B. (2013). CFD simulation of temperature stratification for a building space, Validation and sensitivity analysis. In *13th conference of international building performance simulation association, Chambery, France*.
- Goto, E., & Takakura, T. (1992). Prevention of lettuce tipburn by supplying air to inner leaves. *Transactions of the ASABE*, 35, 641–645.
- Han, J.-H., Kwon, H.-J., Yoon, J.-Y., Kim, K., Nam, S.-W., & Son, J. E. (2009). Analysis of the thermal environment in a mushroom house using sensible heat balance and 3-D computational fluid dynamics. *Biosystems Engineering*, 104(3), 417–424.
- Jiru, T. E., & Bitsuamlak, G. T. (2010). Advances in applications of CFD to natural ventilation. In *The fifth international symposium on computational wind engineering (CWE2010)*. North Carolina, USA: Chapel Hill.
- Jones, J. B. (2005). *Hydroponics – A practical guide for the soilless grower* (2nd ed.). Boca Raton, FL: CRC Press, LCC.
- Kacira, M., Sase, S., & Okushima, L. (2004). Optimization of vent configuration by evaluating greenhouse and plant canopy ventilation rates under wind-induced ventilation. *Transactions of the ASABE*, 47(6), 2059–2067.
- Kim, K., Yoon, J., Kwon, H., Han, J., Son, J. E., Nam, S., et al. (2008). 3-D CFD analysis of relative humidity distribution in greenhouse with a fog cooling system and refrigerative dehumidifiers. *Biosystems Engineering*, 100, 245–255.
- Kitaya, Y. (2005). Importance of air movement for promoting gas and heat exchanges between plants and atmosphere under controlled environments. In K. Omasa, I. Nouchi, & L. J. De Kok (Eds.), *Plant response to air pollution and global change* (pp. 185–193). Tokyo, Japan: Springer-Verlag.
- Kitaya, Y., Tsuruyama, J., Kawai, M., Shibuya, T., & Kiyota, M. (2000). Effects of air current on transpiration and net photosynthetic rates of plants in a closed plant production system. In C. Kubota, & C. Chun (Eds.), *Transplant production in the 21st century* (pp. 83–90). Springer Netherlands Publishers.
- Kitaya, Y., Tsuruyama, J., Shibuya, T., Yoshida, M., & Kiyota, M. (2003). Effects of air current speed on gas exchange in plant leaves and plant canopies. *Advances in Space Research*, 31(1), 177–182.
- Korthals, R. L., Knight, S. L., Christianson, L. L., & Spomer, L. A. (1994). Chambers for studying the effects of airflow velocity on plant growth. *Biotronic*, 23, 113–119.
- Kozai, T. (2013). Plant factory in Japan – current situation and perspectives. *Chronica Horticulturae*, 53(2), 8–11.
- Kozai, T., Chun, C., & Ohyama, K. (2004). Closed systems with lamps for commercial production of transplants using minimal resources. *Acta Horticulturae*, 630, 239–254.
- Lau, J., & Liu, J. L. (2003). Measurement and CFD simulation of the temperature stratification in an atrium using a floor level air supply method. *Indoor and Built Environment*, 12, 265–280.
- Lee, J. G., Choi, C. S., Jang, Y. A., Jang, S. W., Lee, S. G., & Um, Y. C. (2013). Effects of air temperature and air flow rate control on the tipburn occurrences of leaf lettuce in a closed-type plant factory system. *Horticulture Environment and Biotechnology*, 54(4), 303–310.

- Lee, I. B., & Short, T. H. (2000). Two-dimensional numerical simulation of natural ventilation in a multi-span greenhouse. *Transactions of ASAE*, 43(3), 745–753.
- Lim, T.-G., & Kim, Y. H. (2014). Analysis of airflow pattern in plant factory with different inlet and outlet locations using computational fluid dynamics. *Biosystems Engineering*, 39(4), 310–317.
- Majdoubi, H., Boulard, T., Fatnassi, H., & Bouirden, L. (2009). Airflow and microclimate patterns in a one-hectare Canary type greenhouse: an experimental and CFD assisted study. *Agricultural and Forest Meteorology*, 149, 1050–1062.
- Mirade, P. S., & Daudin, J. D. (2006). Computational fluid dynamics prediction and validation of gas circulation in a cheese ripening room. *International Dairy Journal*, 16, 920–930.
- Mistriotis, A., Bot, G. P. A., Picuno, P., & Scarascia-Mugnozza, G. (1997). Analysis of the efficiency of greenhouse ventilation using computational fluid dynamics. *Agricultural and Forest Meteorology*, 85, 217–228.
- Mondaca, M., & Choi, C. Y. (2014). Experimental validation of computational dynamics (CFD) model of perforated polyethylene tube ventilation systems in dairy operations. In *ASABE and CSBE/SCGAB annual international meeting presentation, paper no: 141912797*.
- Norton, T., & Sun, D. W. (2006). Computational fluid dynamics (CFD) – an effective and efficient design and analysis tool for the food industry: a review. *Trends in Food Science & Technology*, 17, 600–620.
- Patankar, S. V. (1980). *Numerical heat transfer and fluid flow*. Washington, WA: Hemisphere Publishing Corporation.
- Posner, J. D., Buchanan, D., & Dunn-Rankin, D. (2003). Measurement and prediction of indoor air flow in a model room. *Energy and Buildings*, 35, 515–526.
- Rohdin, P., & Moshfegh, B. (2007). Numerical predictions of indoor climate in large industrial premises. A comparison between different k-ε models supported by field measurement. *Building and Environment*, 42, 3872–3882.
- Shear, C. B. (1975). Calcium-related disorders of fruits and vegetables. *Hort Science*, 10, 361–365.
- Shibata, T., Iwao, K., & Takano, T. (1995). Effect of vertical air flowing on lettuce growing in a plant factory. *Acta Horticulturae*, 399, 175–183.
- Shibuya, T., & Kozai, T. (1998). Effects of air velocity on net photosynthetic and evapo-transpiration rates of a tomato plug sheet under artificial light. *Environment Control in Biology*, 36, 131–136.
- Shih, T.-H., Liou, W. W., Shabbir, A., Yang, Z., & Zhu, J. (1994). A new k-ε eddy viscosity model for high Reynolds number turbulent flows-model development and validation. *Computers & Fluids*, 24(3), 227–238.
- Tamimi, E., Kacira, M., Choi, C. Y., & An, L. (2013). Analysis of microclimate uniformity in a naturally vented greenhouse with a high-pressure fogging system. *Transactions of the ASABE*, 56(3), 1241–1254.
- Thimijan, R. W., & Heins, R. D. (1983). Photometric, radiometric, and quantum light units of measure, a review of procedures for interconversion. *Journal of the American Society for Horticultural Science*, 18(6), 818–822.
- Weigand, B., & Spring, S. (2009). Multiple jet impingement – a review. *Heat Transfer Research*, 42(2).
- Wells, C., & Amos, N. (1994). Design of air distribution systems for closed greenhouses. *Acta Horticulturae*, 361, 93–102.
- Yabuki, K. (1990). *Wind and photosynthesis. Correspondence of environment of leaf boundary layer and plants* (p. 45). Tokyo, Japan: Nobunkyo Association.